Bull. Mater. Sci., Vol. 37, No. 3, May 2014, pp. 417–423. © Indian Academy of Sciences.

Structural, optical and photoluminescence study of nanocrystalline SnO_2 thin films deposited by spray pyrolysis

AKHILESH TRIPATHI and R K SHUKLA*

Department of Physics, University of Lucknow, Lucknow 226 007, India

MS received 9 January 2013; revised 2 March 2013

Abstract. **Undoped SnO_2 thin films prepared by spray pyrolysis method reveal polycrystalline nature with prominent peaks along (110), (101) and (211) planes. All the films are nanocrystalline with particle size lying in the range of 3·14–8·6 nm calculated by DS formula. Orientation along plane (200) decreases continuously as molar concentration of SnO_2 increases. Dislocation density along plane (110) also decreases as molar concentration increases except 0·4 M SnO_2 thin film. Scanning electron microscopy image of the films contain jelly structures along with agglomerated clusters of particles. SnO_2 synthesized successfully, which confirms by Fourier transform infra-red spectroscopy. The optical transmittance spectra of 0·2 M SnO_2 thin film shows transmittance about 50–60% transmission in visible and near infrared region with a sharp cut off in the ultraviolet region. The transmission decreases in visible and near infrared region as molar concentration increases. Broad UV emission at 398 nm is observed in photoluminescence spectra of the films along with a blue emission, when excited at 250 nm wavelength. Emission intensity randomly changed as SnO_2 molar concentration increases. When excited at 320 nm, one UV and two visible peaks appeared at 385, 460 and 485 nm, respectively.**

Keywords. **SnO_2; thin films; X-ray diffraction; optical transmission; photoluminescence study.**

1. Introduction

Rutile type SnO_2 is an important semiconductor because of its dipole forbidden direct band gap of 3·6 eV at room temperature (Vijayalakshmi *et al* 2008; Rozati and Shadmani 2010). The study of SnO_2 transparent conducting oxide thin films are of great interest due to its unique attractive properties like high optical transmittance, uniformity, nontoxicity, good electrical, low resistivity, stability to heat treatment, mechanical hardness, piezoelectric behaviour and its low cost. SnO_2 thin films have vast applications as window layers, heat reflectors in solar cells, flat panel display, electro-chromic devices, LEDs, liquid crystal displays, invisible security circuits, various gas sensors, etc. For many of these applications, it is advantageous to use tin oxide in thin film form and this can be accomplished in different ways (Elam *et al* 2008; Vadivel *et al* 2011; Zhang *et al* 2011).

The advancement in nanostructured oxides has attracted new interest in exploiting these materials as components for nano scale light emitting devices (He *et al* 2006). Besides other material properties, photoluminescence (PL) properties of SnO_2 can be manipulated by varying the size, defects such as tin interstitials or oxygen vacancies, which act as radiative centres in luminescence process (Jeong *et al* 2003; Morais *et al* 2006). Thin films of SnO_2 can be prepared by many techniques, such as chemical vapour deposition, sputtering, sol–gel spin coating, reactive evaporation, pulsed laser ablation, screen printing technique, spray pyrolysis, etc. Among these techniques, spray pyrolysis is the most convenient method because of its simplicity, low cost, ease to add dopants and facility to vary the film properties by changing composition of precursor solution. In addition, this method is promising for high rate and mass production capability of uniform large area coatings in industry (Zhang *et al* 2011).

However, the PL origin is not clear due to its sensitivity to surface states (Xiang *et al* 2008). The PL spectrum of SnO_2 shows the red and blue emission for nanorods, nanoribbons, nanoparticles, etc. (Her *et al* 2006; Moon *et al* 2007). The particle size of the nanocrystalline SnO_2 is small enough to increase the active surface of the particles and materials (Chen *et al* 2009; Torabi and Sadrnezhaad 2011). Very few reports have been published regarding the UV emission of SnO_2, especially for nanomaterials (Gu *et al* 2003; Liu *et al* 2006). In this investigation, SnO_2 thin films were deposited with various molar concentrations because PL is also sensitive to surface states.

Here, we have deposited thin films by spray pyrolysis method. Structural properties are studied by X-ray diffraction (XRD) and Fourier–transform infrared (FT–IR)

*Author for correspondence (rajeshkumarshukla_100@yahoo.co.in)

spectroscopy. Morphological properties are studied by scanning electron microscopy (SEM). The transmission and photoluminescence (PL) spectra have been recorded to analyse optical properties.

2. Experimental

2.1 *Thin film preparation*

In the present work, the precursor solution has been prepared for obtaining pure SnO_2 films by dissolving predetermined amount of tin chloride ($SnCl_4{\cdot}5H_2O$) in methanol and diethanolamine to form 0·2, 0·4, 0·6 and 0·8 molar solutions. The mixture is then magnetically stirred at 40 °C for half an hour to get a homogeneous solution. All the solutions are aged for one month to achieve proper viscosity and stability. The films are prepared by spray pyrolysis method of all the precursor solutions. Prior to film deposition, the slides of glass substrates were properly cleaned in an ultrasonic cleaner using methanol, acetone and de-ionized water.

The experimental set-up of spray pyrolysis contains glass atomizer for spraying the precursor solution. The substrates are kept on hot iron plate which is already attached with thermocouple and temperature controller to maintain the required temperature. The precursor solution to be sprayed is introduced in the solution container which is connected to the liquid inlet of the atomizer by a tube which has a solution flow controller. Compressed air used as carrier gas, is let into the gas inlet of the atomizer after passing through a pressure gauge.

First, for the preparation of thin films by spray pyrolysis, 10 mL volume of the precursor solution of each sample, one at a time is transferred to the solution container. The distance between nozzle and the substrate is set at 25 cm and the flow rate is 1 mL/min. The substrate temperature is maintained at 450 °C to obtain good quality films. Post deposition annealing of the films are done at 450 °C for 4 h. In this way, first four samples are prepared: 0·2, 0·4, 0·6 and 0·8 M SnO_2 thin films. Here, these samples prepared by spray pyrolysis method are referred as samples 1, 2, 3 and 4, respectively.

2.2 *Characterizations*

The XRD spectra of all the samples recorded by Phillips X'pert PW3020 diffractometer using CuKα radiation (λ = 1·54056 Å) are presented for structural analysis of the samples. The SEM images of all the thin films are taken by scanning electron microscope (Model-430, LEO Cambridge, England). FT–IR spectra of all the thin films are recorded on the Bruker Alpha spectrometer to determine the formation of polyaniline. Then, the optical transmission spectra of the films are recorded with UV-Vis spectrophotometer (Model no. V-670 Jasco). Photoluminescence spectra are recorded with photoluminescence spectrophotometer (LS-55, Perkin Elmer fluorescence spectrometer) at two excitation (λ_{exc}) wavelengths of 250 and 320 nm. The incident excitation density is controlled by using calibrated neutral density filters in front of the spectrometer slit. The slit widths for emission spectra recording have been chosen as 10 nm. The excitation source is a 20 kW xenon discharge lamp. The light beam used for excitation is focused on the film surface in circular area of diameter ~ 5 nm.

3. Results and discussion

3.1 *XRD studies*

The XRD spectra of all the samples recorded by Phillips X'pert PW3020 diffractometer using CuKα radiation (λ = 1·54056 Å) were presented for structural analysis of the samples. The XRD patterns of the as-prepared samples 1, 2, 3 and 4, i.e. 0·2, 0·4, 0·6 and 0·8 M thin films are shown in figure 1. Four peaks along (110), (101), (200) and (211) planes are clearly observed which indicate that the films are polycrystalline in nature. However, intensity of the peak along (200) plane is very small in 0·2 M thin film which decreases as molar concentration increases and vanishes for higher molar concentration. All the diffraction lines are assigned to tetragonal rutile crystalline phases of tin oxide. No characteristic peaks of impurities were observed.

Using the back ground noise level as a reference, the (*hkl*) orientation parameters $\gamma_{(hkl)}$ is calculated from the relative heights of (110), (101), (200) and (211) reflection peaks using the following expression and are given in table 1 (Srivastava *et al* 2011)

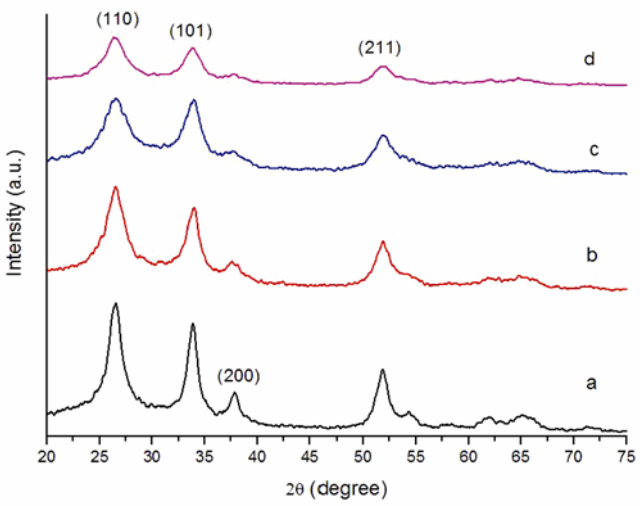

Figure 1. XRD spectra of samples 1, 2, 3 and 4. Images (a), (b), (c) and (d) correspond to samples 1, 2, 3 and 4, respectively i.e. SnO_2 thin films of 0·2, 0·4, 0·6 and 0·8 M precursors.

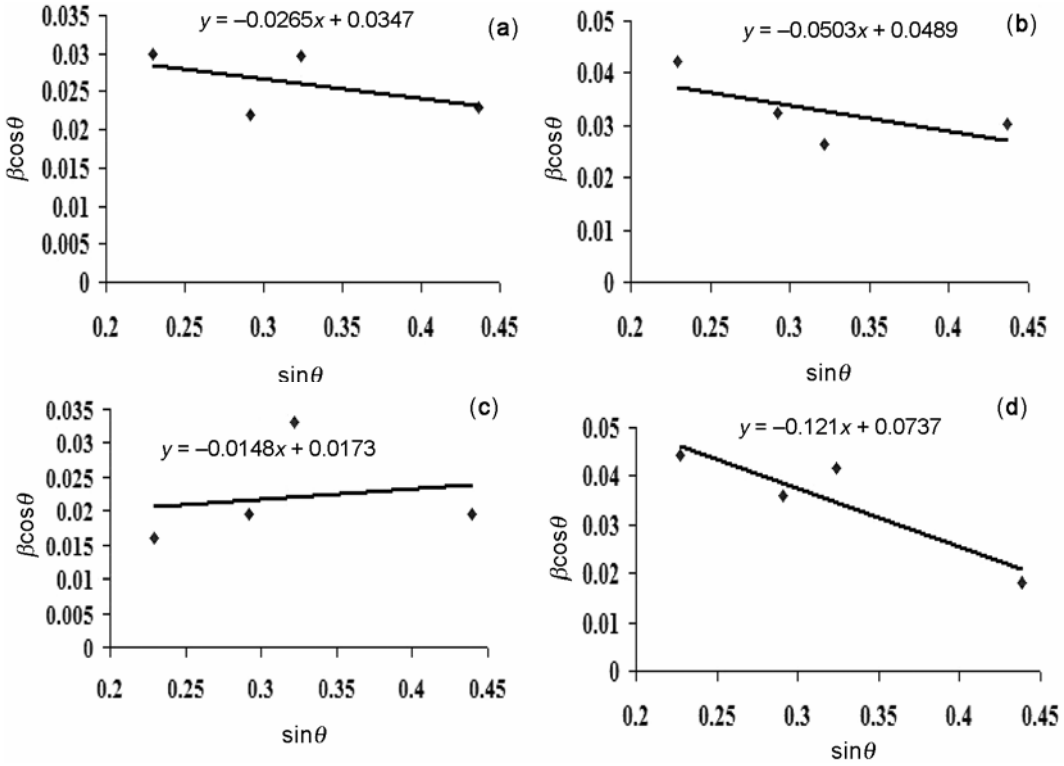

Figure 2. Williamson–Hall plots of samples 1, 2, 3 and 4. Images (**a**), (**b**), (**c**) and (**d**) correspond to samples 1, 2, 3 and 4, respectively i.e. SnO_2 thin films of 0·2, 0·4, 0·6 and 0·8 M precursors.

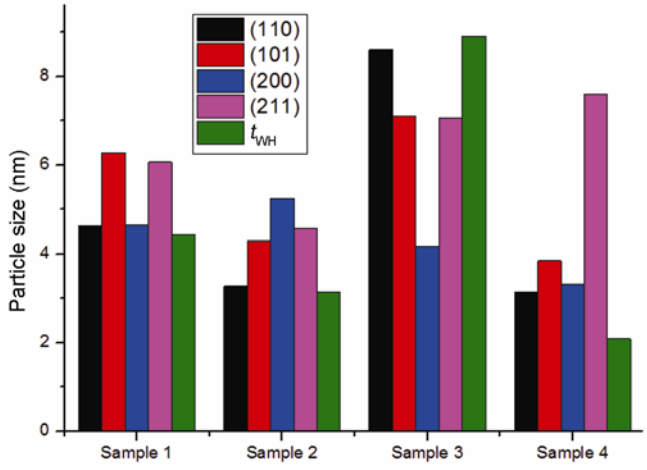

Figure 3. Comparison of particle size calculated by DS formula along each plane (110), (101), (200) and (211) and WH plot of all samples.

Table 1. Orientation parameter $\gamma_{(hkl)}$ of samples 1–4.

	Orientation parameter (γ)			
Sample	(110)	(101)	(200)	(211)
1	0·380	0·319	0·115	0·183
2	0·394	0·312	0·108	0·184
3	0·360	0·352	0·108	0·178
4	0·418	0·326	0·092	0·161

$$\gamma_{(hkl)} = \frac{I_{(hkl)}}{I_{(110)} + I_{(101)} + I_{(200)} + I_{(211)}}. \quad (1)$$

From the table, random orientation of samples is obvious. Orientation parameter is maximum for (110) plane of each sample and minimum for (200) plane. Orientation parameter decreases for plane (200) as molar concentration of SnO_2 increases.

The particle size in the samples is estimated using Debye Scherrer's formula (2) (Misra *et al* 2009).

$$t_{DS} = \frac{k\lambda}{\beta \cos\theta}, \quad (2)$$

where t_{DS} is particle diameter, k the Scherer constant and is taken equal to 1, λ the wavelength of X-rays, β the full-width at half-maximum (FWHM) of X-ray diffraction peaks in radians. Particle size for all the samples along each crystallographic plane as determined by DS formula, is summarized in table 2. All the films are nanocrystalline with particle size lying between 3·14 and 8·6 nm.

3.1a *Williamson and Hall analysis*: In order to distinguish the effect of crystallite size-induced broadening and strain-induced broadening of FWHM of XRD peaks, the Williamson and Hall (WH) plot has been performed and shown in figure 2.

Table 2. Particle size as determined by DS formula and WH plot and strain in samples 1–4.

Sample	Particle size (t_{DS}) in nm (110)	(101)	(200)	(211)	t_{WH} (nm)	Strain (ε_0)
1	4·63	6·28	4·65	6·07	4·44	$-1{\cdot}32 \times 10^{-2}$
2	3·28	4·30	5·25	4·57	3·15	$-2{\cdot}51 \times 10^{-2}$
3	8·60	7·10	4·18	7·06	8·91	$7{\cdot}40 \times 10^{-3}$
4	3·14	3·85	3·33	7·60	2·09	$-6{\cdot}05 \times 10^{-2}$

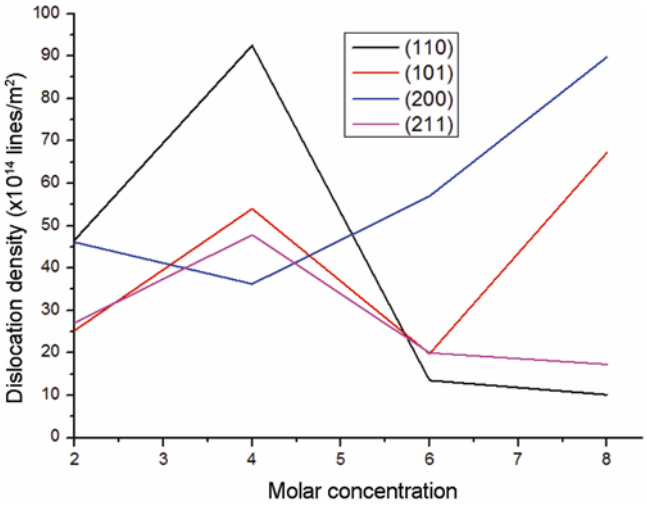

Figure 4. Variation of dislocation density with molar concentration along (110), (101), (200) and (211) plane.

The particle size and strain are obtained by comparing trend line with (3) (Misra *et al* 2009).

$$\beta \cos\theta = \frac{C\lambda}{t_{WH}} + 2\varepsilon \sin\theta, \tag{3}$$

where t_{WH} is the particle size, ε the strain and C the correction factor which is taken as 1. The strain and the particle size thus determined are summarized in table 2.

Here, the strain is of compressive nature for all the samples which is indicated by its negative sign except sample 3, i.e. 0·6 M SnO_2 thin film. Therefore for all the samples, the particle size obtained from DS formula nearly matches with that obtained by WH plot as shown in figure 3.

The dislocation density (δ), which represents the amount of defects in the film, is calculated using (4) (Khan *et al* 2011).

$$\delta = \frac{1}{t_{DS}^2}, \tag{4}$$

where t_{DS} is particle size calculated using DS formula. The calculated values of dislocation density (δ) are randomly vary between $10{\cdot}12 \times 10^{14}$ and $92{\cdot}53 \times 10^{14}$ lines/m^2 for all the samples along each plane and is shown in table 3. Dislocation density decreases along plane (110) and (211) as molar concentration increases except for sample 2, i.e. 0·4 M SnO_2 thin film as shown in figure 4.

3.2 *SEM studies*

The study of surface morphology of SnO_2 thin films deposited by spray pyrolysis method has been carried out using scanning electron microscope (Model no. LEO-430, Make-LEO Cambridge-England). In figure 5, images (a), (b), (c) and (d) present SEM of the samples 1, 2, 3 and 4, respectively, which is prepared by spray pyrolysis method. As can be seen in the figure, jelly structures are formed along with agglomerated clusters of particles. With increase in molar concentration, the network of jelly seem to expand due to lack of cohesion among the film particles.

3.3 *FT–IR studies*

The FT–IR transmission spectra of samples were taken with the help of FT–IR spectrometer (Model Alpha Bruker) as shown in figure 6. The Sn–O–Sn vibration appeared in the range of 400–700 cm^{-1} as the result of condensation reaction (Patil *et al* 2003; Singh *et al* 2012). The peaks around 539 cm^{-1} are assigned to the asymmetric Sn–O–Sn stretching mode of the surface-bridging oxide formed by the condensation of adjacent surface hydroxyl groups. The spectra changes can be easily attributed to changes in size and shape of the SnO_2 particles (Gu *et al* 2003). The absorption peaks are appeared in the region of 750–850 cm^{-1} due to Sn–O stretching vibration in all the samples. The peaks around 1356 cm^{-1} are appeared due to symmetric and asymmetric stretching vibrations of the SnO_2 film (Amalric-Popescu and Bozon-Verduraz 2001). The absorption peaks in the region of 1600–1700 cm^{-1} are attributed to vibration of hydroxyl due to the fact that SnO_2 retained certain adsorbed water (Fang *et al* 2008).

3.4 *Optical transmission*

The optical transmission of the samples is investigated in the range of 300–900 nm using UV–Vis spectrophotometer

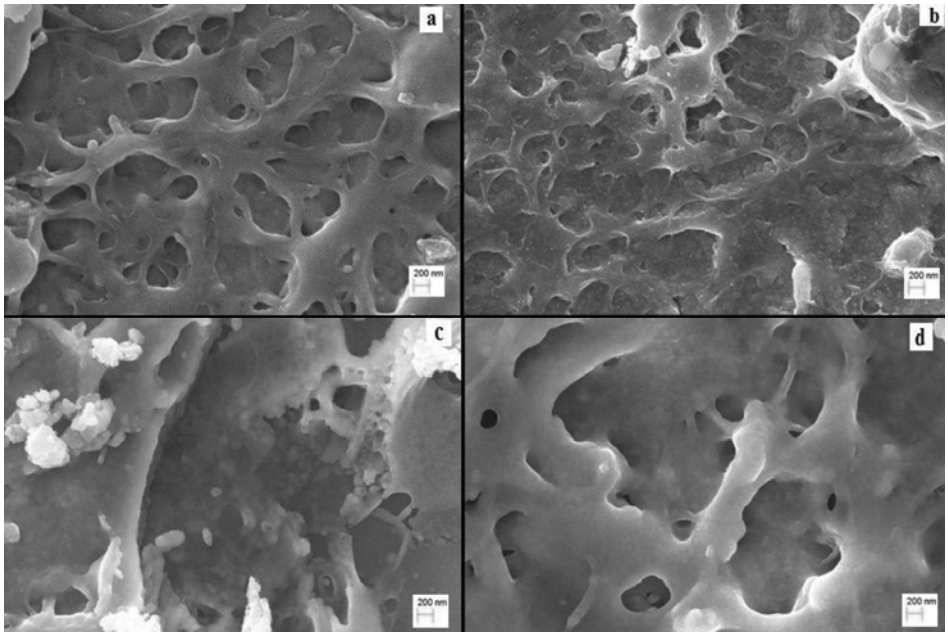

Figure 5. SEM images of samples 1, 2, 3 and 4. Images (**a**), (**b**), (**c**) and (**d**) correspond to samples 1, 2, 3 and 4, respectively i.e. SnO_2 thin films of 0·2, 0·4, 0·6 and 0·8 M precursors.

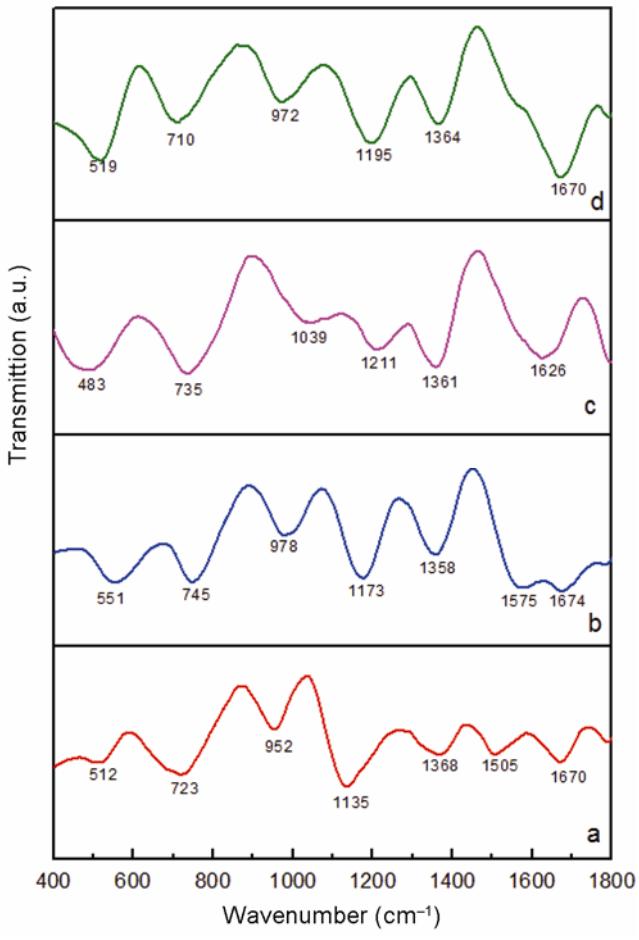

Figure 6. FT–IR spectra of samples 1, 2, 3 and 4. Curves (**a**), (**b**), (**c**) and (**d**) correspond to samples 1, 2, 3, and 4, respectively i.e. SnO_2 thin films of 0·2, 0·4, 0·6 and 0·8 M precursors.

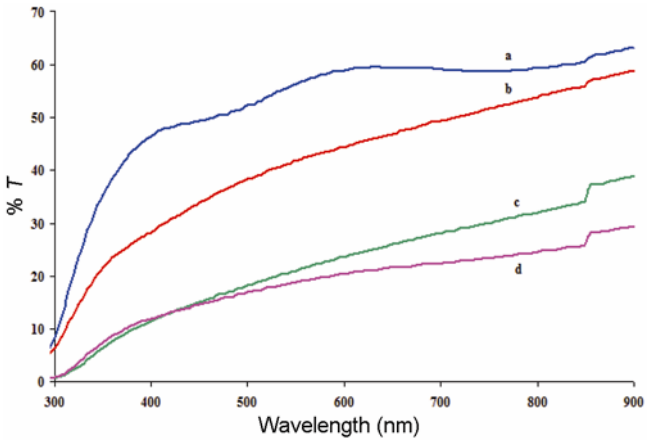

Figure 7. Transmission spectra of samples 1, 2, 3 and 4. Curves a, b, c and d correspond to samples 1, 2, 3 and 4, respectively i.e. SnO_2 thin films of 0·2, 0·4, 0·6 and 0·8 M precursors.

Table 3. Dislocation density of samples 1–4.

	Dislocation density (δ) $\times 10^{14}$ (lines/m^2)			
Sample	(110)	(101)	(200)	(211)
1	46·64	25·31	46·11	27·09
2	92·53	53·99	36·26	47·81
3	13·51	19·80	56·96	20·01
4	10·12	67·25	89·78	17·30

(Model no. V-670 Jasco) as shown in figure 7. The measurements are taken in the wavelength scanning mode for normal incidence. Transmission spectra show 50–60% transmission in visible and near infrared region with a

sharp cut off in the ultraviolet region for sample 1, i.e. 0·2 M thin film. The transmission decreases in visible and near infrared region as molar concentration increases and reaches up to 10–15% transmission.

3.5 *PL studies*

PL spectra were recorded at two excitation wavelengths 250 and 320 nm as shown in figures 8 and 9, respectively. PL spectra of same samples show broad UV and low intense visible peaks about at 398 and 476 nm, respectively, when excited at 250 nm. This is similar to the result reported by Gu *et al* (2003). When excited at 320 nm, one UV and two visible peaks appeared at 385, 460 and 485 nm, respectively. Both UV and visible peaks shift towards lower value when excited at 320 nm compared to peak position in spectra at excitation wavelength 250 nm and a new peak in visible region at 485 nm was found. Peaks in the UV and visible region do not shift, but there is a random change in their intensities for both excitation wavelengths. Since the energy of excitation and emission both are lower than the band gap of SnO_2 ($E_g = 3{\cdot}56$ eV), therefore emission seems not due to the direct recombination of a conduction electron in the 4*p* band of Sn and a hole in the 2*p* valence band of O. A weak peak at 3·13 eV emitted from undoped SnO_2 at low temperature, and room temperature, is reported by Kim *et al* (2000). They have related the origin of both the peaks to defects or to defect levels associated with oxygen vacancies or nanocrystal grains or tin interstitials resulting from the nano-size of the SnO_2 thin film. Emission intensity of both the peaks at excitation wavelength 320 nm diminishes by increasing the molar concentration of SnO_2. The reason behind this decrement of intensity may be molar concentration variation or particle size reduction or both as nanosize dependent PL is reported by Lee *et al* (2004).

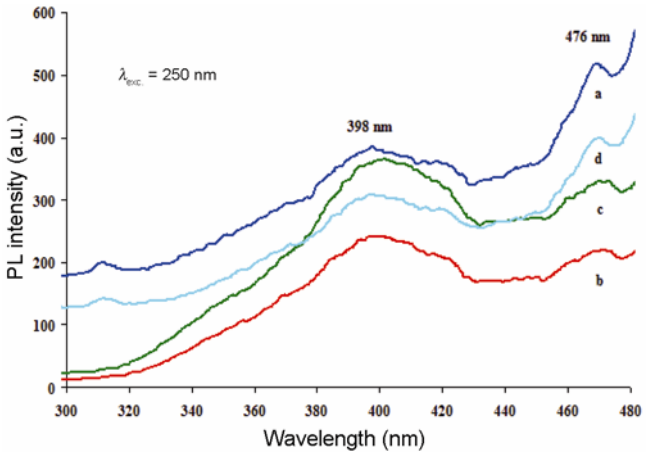

Figure 8. PL spectra of samples 1, 2, 3 and 4 at excitation wavelength of 250 nm. Curves a, b, c and d correspond to samples 1, 2, 3 and 4, respectively i.e. SnO_2 thin films of 0·2, 0·4, 0·6 and 0·8 M precursors.

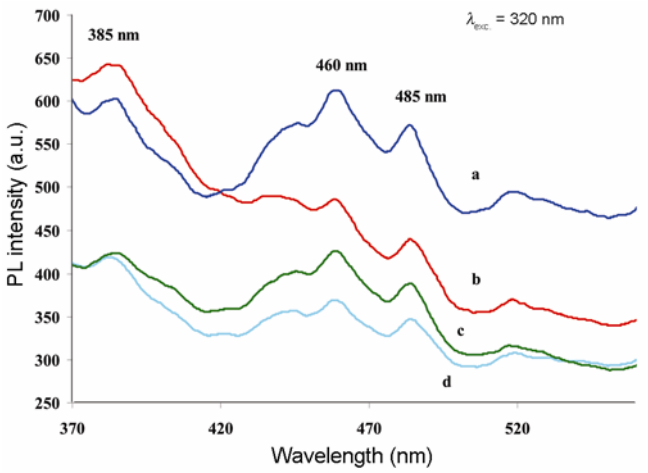

Figure 9. PL spectra of samples 1, 2, 3 and 4 at excitation wavelength of 320 nm. Curves a, b, c and d correspond to samples 1, 2, 3 and 4, respectively i.e. SnO_2 thin films of 0·2, 0·4, 0·6 and 0·8 M precursors.

4. Conclusions

In brief, SnO_2 films of various molar concentrations are prepared by spray pyrolysis method. XRD spectra reveal polycrystalline nature of the films. Three major peaks along (110), (101) and (211) planes are clearly seen, which indicate the tetragonal rutile structure. The particle size calculated by DS formula lies between the ranges 3·14 and 8·6 nm. The particle size calculated by DS formula and WH plot are nearly same. Surface morphology is studied by scanning electron microscopy. SnO_2 has been successfully synthesized from hydrated tin chloride and its formation is confirmed by FT–IR study. Transmission spectra show 50–60% transmission in visible and near infrared regions with a sharp cut off in the ultraviolet region for sample 1, i.e. 0·2 M thin film. It decreases as molar concentration increases. PL spectra of same samples show broad UV and low intense visible peaks about at 398 and 476 nm, respectively, when excited at 250 nm. When excited at 320 nm, one UV and two visible peaks appeared at 385, 460 and 485 nm, respectively.

Acknowledgements

Financial assistance from DST, New Delhi, India vide project no. SR/S2/CMP-004/2009 and Special Assistance Programme (SAP), UGC, New Delhi is gratefully acknowledged.

References

Amalric-Popescu D and Bozon-Verduraz F 2001 *Catalysis Today* **70** 139

Chen H T, Wu X L, Xiong S J, Zhang W C and Zhu 2009 *J. Appl. Phys.* **A97** 365

Elam Jeffrey W, Baker David A, Hryn Alexander J, Martinson Alex B F, Pellin Michael J and Joseph T H 2008 *J. Vac. Sci. Technol.* **A26** 2

Fang L M, Zu X T, Li Z J, Zhu S, Liu C M, Zhou W L and Wang L M 2008 *J. Alloys Compds.* **454** 261

Gu F, Wang S F, Lu M K, Qi Y X, Zhou G J, Xu D and Yuan D R 2003 *Inorg. Chem. Commun.* **6** 882

Gu F, Wang S F, Song C F, Lu M K, Qi X Y, Zhou G J, Xu D and Yuan D R 2003 *Chem. Phys. Lett.* **372** 451

He Jr H, Wu Te H, Hsin C L, Li K M, Chen L J, Chueh Y L, Chou L J and Wang Z L 2006 *Small* **2** 116

Her Y C, Wu J Y, Lin Y R and Tsai S Y 2006 *Appl. Phys. Lett.* **89** 043115

Jeong J, Choi S P, Chang C I, Shin D C, Park J S, Lee B T, Park Y J and Song H 2003 *J. Solid State Commun.* **127** 595

Khan Z R, Khan M S, Zulfequar M and Khan M S 2011 *Mater. Sci. Appl.* **2** 340

Kim T W, Lee D U and Yoon Y S 2000 *J. Appl. Phys.* **88** 3759

Lee E J H, Ribeiro C, Giraldi T R, Longo E, Leite E R and Varela J A 2004 *Appl. Phys. Lett.* **84** 1745

Liu C M, Zu X T, Wei Q M and Wang L M 2006 *J. Phys. D: Appl. Phys.* **39** 2494

Misra K P, Shukla R K, Srivastava A and Srivastava A 2009 *Appl. Phys. Lett.* **95** 031901

Moon T, Hwang S T, Jung D R, Son D, Kim C, Kim J, Kang M and Park B 2007 *J. Phys. Chem.* **C111** 4164

Morais E A D, Scalvi L V A, Martins M R and Ribeiro S J L 2006 *Braz. J. Phys.* **36** 270

Patil P S, Kawar R K, Seth T, Amalnerkar D P and Chigare P S 2003 *Ceram. Int.* **29** 725

Rozati S M and Shadmani E 2010 *Surf. Interf. Anal.* **42** 1160

Singh M K, Mathpal M C and Agarwal A 2012 *Chem. Phys. Lett.* **536** 87

Srivastava A, Shukla R K and Misra K P 2011 *Cryst. Res. Technol.* **46** 949

Torabi M and Sadrnezhaad S K 2011 *J. Power Sources* **196** 399

Vadivel K, Arivazhagan V and Rajesh S 2011 *Int. J. Sci. & Eng. Res.* **2** 4

Vijayalakshmi S, Venkataraj S, Subramanian M and Jayavel R 2008 *J. Phys. D: Appl. Phys.* **41** 035505

Xiang X, Zu X T, Zhu S L, Wang M, Shutthanandan V, Nachimuthu P and Zhang Y 2008 *J. Phys. D: Appl. Phys.* **41** 225102

Zhang B, Tian Y, Zhang J X and Cai W 2011 *J. Optoelectron. Adv. Mater.* **13** 89